

Spin relaxation in cubic III-V semiconductor low-dimensional structures via the interaction with polar-optical phonons

A. Dyson and B. K. Ridley

Department of Electronic Systems Engineering, University of Essex, Colchester CO4 3SQ, United Kingdom

(Received 17 May 2004; published 14 July 2005)

Spin-relaxation rates have been calculated for the D'yakonov-Perel (DP) mechanism involving the interaction with polar-optical phonons. The inelastic nature of the collisions has been fully taken into account and expressions for the energy-dependent time constants have been found for arbitrary degeneracy and for both strong and weak spin-population differences. We investigate the energy and temperature dependence of the spin-relaxation rates for a range of quantum well (QW) widths and quantum wire (QWR) cross sections. The spin-relaxation time is found to exhibit a monotonic temperature dependence and an E^{-2} dependence on subband energy.

DOI: [10.1103/PhysRevB.72.045326](https://doi.org/10.1103/PhysRevB.72.045326)

PACS number(s): 72.25.Rb, 72.10.Di

I. INTRODUCTION

There is considerable interest in spin-polarized dynamics in quantum confined structures currently, due to the many proposed spintronic devices. For the most part, interest has focused on spin-relaxation rates in quantum wells of III-V semiconductors. Due to the ease with which a spin-polarized population may be generated by selective optical pumping. The D'yakonov-Perel (DP)¹ mechanism extended to quantum wells² is highlighted as being dominant in GaAs at room temperature.³⁻⁵ One-dimensional confinement suppresses spin-relaxation. A symmetric quantum wire (QWR) with a single subband preserves spin polarization, even if there is significant spin-orbit coupling due either to bulk (Dresselhaus) or structural (Rashba) inversion asymmetry.⁶ In an asymmetric wire, spin relaxation will proceed via the DP mechanism assuming spin-orbit coupling due to bulk inversion asymmetry is present. At room temperature in III-V compound semiconductors such as GaAs the DP mechanism is dominant for spin relaxation and the most powerful scattering mechanism in is polar-optical-phonon (POP) scattering. The presence of scattering will enhance spin relaxation via the DP mechanism. Spin relaxation in QWR's has been studied with the aid of Monte Carlo simulations.^{7,8} While both of these reports consider POP the former limit themselves to elastic collisions and the latter consider temperatures below 50 K only. Motivated by the ultimate goal of room temperature devices, we have examined the DP mechanism in two-dimensional (2D) and one-dimensional (1D) taking the inelastic nature of the POP scattering fully into account.

The profoundly inelastic nature of the interaction means that a simple momentum-relaxation time cannot be defined and standard formulas for relaxation rates found in the literature cannot be used. The problem is well known in transport theory where various techniques have been employed to solve the Boltzmann equation either approximately or numerically. However, in principle an exact solution of the Boltzmann equation can be obtained by using a ladder technique^{9,10} in which the energy rungs of the ladder are separated by a phonon energy. Starting at a high energy

where a momentum-relaxation time constant can be defined, one can use the ladder technique to define a time constant for the lowest rung. Repetition of the technique yields the time constant for the next lowest rung, and so on for the higher rungs. Recently this technique has been used in the case of bulk GaN,¹¹ AlGaIn/GaN heterostructure¹² and by us for bulk¹³ DP mechanism.

The paper is organized as follows: Section II describes the Hamiltonian for the DP mechanism, Sec. III describes the 2D case, Sec. IV the 1D case, and Sec. V presents the results and discussion for both.

II. THE D'YAKONOV-PEREL MECHANISM

The conduction-band Hamiltonian is of the form:

$$H = \frac{\mathbf{k}^2}{2m^*} + \frac{\hbar}{2}(\boldsymbol{\sigma} \cdot \boldsymbol{\Omega}(\mathbf{k})), \quad \boldsymbol{\Omega}(\mathbf{k}) = \gamma \boldsymbol{\kappa} \quad (1)$$

$$\gamma^2 = \frac{2}{9} \frac{\eta^2}{(1+\eta)\left(1+\frac{2}{3}\eta\right)} \left(\frac{1}{m^*} - \frac{1}{m}\right) \frac{B^2}{E_g} \quad \eta = \frac{\Delta_0}{E_g} \quad (2)$$

where \mathbf{k} is a two-dimensional momentum in the plane, γ is the bulk spin splitting coefficient,¹⁴ $\boldsymbol{\sigma}$ are the Pauli matrices, m^* is the effective mass, m is the free-electron mass, E_g is the band gap, Δ_0 is the spin-orbit splitting, and B is the matrix element describing the interaction with the second subband. In the D'yakonov-Perel mechanism $\boldsymbol{\kappa}$ is interpreted as a vector defining the direction of an effective magnetic field and $\boldsymbol{\Omega}$ is then the precession frequency of the spin. Precession itself does not relax all components of spin; collisions are required that change the direction of $\boldsymbol{\kappa}$. The operative time is the momentum-relaxation time τ_p , as distinct from the scattering time, associated with the scattering mechanism. When $\boldsymbol{\Omega}\tau_p \gg 1$ the spin relaxes before a scattering event can take place. Typically, however, the spin-splitting of the conduction band is very small and the scattering time is very short and so $\boldsymbol{\Omega}\tau_p \ll 1$. In this paper we are only concerned with the contribution coming from polar-optical phonon scattering

III. QUANTUM WELLS

The components of the precession frequency of the spin are:

$$\Omega_x = \gamma k_x (k_y^2 - k_z^2), \quad \Omega_y = \gamma k_y (k_z^2 - k_x^2), \quad \Omega_z = \gamma k_z (k_x^2 - k_y^2) \quad (3)$$

Taking the confinement direction to be along z we can replace $\langle k_z^2 \rangle$ with K_i^2 by taking the expectation value.

$\Omega_x = \gamma k_x (k_y^2 - K_i^2)$, $\Omega_y = \gamma k_y (K_i^2 - k_x^2)$, $\langle \Omega_z \rangle = 0$ where i is the subband index. Thus we have:¹¹

$$\Omega_x = -\Omega_1 \cos \alpha - \Omega_3 \cos 3\alpha \quad (4)$$

$$\Omega_y = \Omega_1 \sin \alpha - \Omega_3 \sin 3\alpha$$

$$\Omega_1 = \gamma k \left(K_i^2 - \frac{k^2}{4} \right), \quad \Omega_3 = \gamma \frac{k^3}{4}, \quad \tan \alpha = \frac{k_y}{k_x}$$

Scattering takes \mathbf{k} to \mathbf{k}' and K_i to K_j . For simplicity we consider only intrasubband transitions, on the assumption that higher bands will not be occupied. This assumption is valid since the energy separation to the next lowest subband is ~ 10 kT. The tensor components of the scattering times are obtained by first considering \mathbf{k} to be along the x direction. The scattered component is:

$$\Omega'_x = -\Omega'_1 \cos \theta - \Omega'_3 \cos 3\theta \quad (5)$$

where θ is the scattering angle. Similarly the y component is:

$$\Omega'_y = \Omega'_1 \cos \theta + \Omega'_3 \cos 3\theta \quad (6)$$

We now have two time constants one associated with θ the other with 3θ .

This situation is conveniently described using spin-density-matrix methods.¹⁵ The method has already been employed by us to analyze the bulk.¹³

It is common to limit our discussion to those scattering mechanisms involving elastic collisions, but this is not possible when the interaction is with optical phonons, except in the unrealistic high-energy limit when $E \gg \hbar\omega$. In most cases (and temperatures) of practical interest E is less than or of the order of the phonon energy, thus we must take into account separately the role of absorption and emission processes. Taking into account occupation probabilities and degeneracy we then have:

$$\begin{aligned} & i \frac{1}{\hbar} [H_1(\mathbf{k}, \bar{\rho}) + \sum_{\mathbf{k}'} W_{\mathbf{k}\mathbf{k}'}^{abs} \left\{ (n+1) \frac{f_0(E + \hbar\omega)}{f_0(E)} \rho_1(\mathbf{k}) \right. \\ & \left. - n \frac{f_0(E)}{f_0(E + \hbar\omega)} \rho_1(\mathbf{k}') \right\} + \sum_{\mathbf{k}''} W_{\mathbf{k}\mathbf{k}''}^{em} \left\{ n \frac{f_0(E)}{f_0(E - \hbar\omega)} \rho_1(\mathbf{k}) \right. \\ & \left. - (n+1) \frac{f_0(E - \hbar\omega)}{f_0(E)} \rho_1(\mathbf{k}'') \right\} = 0. \end{aligned} \quad (7)$$

The spin density, $\rho(\mathbf{k})$ is defined as $\bar{\rho} + \rho_1(\mathbf{k})$ and the bar denotes an average over all directions of \mathbf{k} , n is the phonon occupation number, $H_1(\mathbf{k}) = \frac{1}{2} \hbar (\boldsymbol{\sigma} \cdot \boldsymbol{\Omega}(\mathbf{k}))$ and assuming solutions of the form $\rho_1(\mathbf{k}) = -i [\boldsymbol{\tau}^*(E)/\hbar][H_1(\mathbf{k}), \bar{\rho}]$.

Connection is thereby made to states $E - \hbar\omega$ and $E + \hbar\omega$ and from these states to more remote states. Since it is not possible to define an overall momentum-relaxation we define an energy-dependent time constant $\tau^*(E)$ associated with each of the directionally dependent terms in analogy with the corresponding solution of the Boltzmann equation for optical mode scattering.

Using the properties of the spin operator we can evaluate the commutator in Eq. (7) and obtain the rate of decay of a spin component:

$$\frac{ds_x}{dt} = -\tau^*(E) \{s_x(\Omega_y^2 + \Omega_z^2) - s_y \Omega_x \Omega_y - s_z \Omega_x \Omega_z\} \quad (8)$$

As Pikus and Titkov¹⁵ have pointed out, the rate is a tensor quantity that reduces to a scalar when an average over direction is taken since

$$\overline{\Omega_i \Omega_j} = 0, \quad i \neq j, \quad \text{and} \quad \overline{\Omega_x^2} = \overline{\Omega_y^2} = (\overline{\Omega_1^2} + \overline{\Omega_3^2}), \quad \overline{\Omega_z^2} = 0 \quad (9)$$

$$\frac{1}{T_z} = \frac{2}{T_{x,y}} = 2(\Omega_1^2 \tau_1 + \Omega_3^2 \tau_3) \quad (10)$$

We now need to determine $\tau^*(E)$ from Eq. (7), substitution of expressions for $H_1(\mathbf{k})$, $\rho_1(\mathbf{k})$ and ρ gives Eq. (11).

$$\begin{aligned} & \sum_{\mathbf{k}'} W_{\mathbf{k}\mathbf{k}'}^{abs} \left\{ (n+1) \frac{f_0(E + \hbar\omega)}{f_0(E)} \tau_p^*(E) \right. \\ & \left. - n \frac{f_0(E)}{f_0(E + \hbar\omega)} \lambda_p' \tau_p^*(E') \cos p\beta' \right\} \\ & + \sum_{\mathbf{k}''} W_{\mathbf{k}\mathbf{k}''}^{em} \left\{ n \frac{f_0(E - \hbar\omega)}{f_0(E)} \tau_p^*(E) - (n+1) \right. \\ & \left. \times \frac{f_0(E)}{f_0(E - \hbar\omega)} \lambda_p'' \tau_p^*(E'') \cos p\beta'' \right\} = 1. \end{aligned} \quad (11)$$

where

$$\lambda_p' = \Omega_p' / \Omega_p,$$

$$\cos \beta' = [1 - (q^2/2k^2) + (\hbar\omega/2E)] / \sqrt{1 + (\hbar\omega/E)},$$

$$\cos \beta'' = [1 - (q^2/2k^2) - (\hbar\omega/2E)] / \sqrt{1 - (\hbar\omega/E)}$$

with $p=1$ or 3 . The effective time constants are obtained from the coupled equations:

$$A'(E) \tau^*(E + \hbar\omega) + B'(E) \tau^*(E - \hbar\omega) + C'(E) \tau^*(E) = 1 \quad (12)$$

with $E = \xi + m\hbar\omega$, $0 < \xi < \hbar\omega$ and $m=0, 1, 2$, etc. and $A'(E)$, $B'(E)$, and $C'(E)$ are the relevant collision integrals (see the Appendix). For m sufficiently large ($E \gg \hbar\omega$) a time-constant can be defined and then used to solve for all the lower energy time-constants. Matrix inversion techniques are employed to solve the set of m equations.

IV. QUANTUM WIRES

Taking the confinement directions to be along x and y results in scattering along the wire either forward or backward in z . Again we limit ourselves to intrasubband scattering due to the large energy separation to the next subband. The minimum energy gap for the widest wire considered is ~ 3 kT. The expectation values are $\langle k_x^2 \rangle = K_i^2$ and $\langle k_y^2 \rangle = \Lambda_j^2$ with i and j the subband indices.

$$\overline{\Omega_i \Omega_j} = 0, \quad i \neq j, \quad \text{and} \quad \overline{\Omega_x^2} = \overline{\Omega_y^2} = 0, \quad \overline{\Omega_z^2} = [\gamma k_z (K_i - \Lambda_j)]^2 \quad (13)$$

$$\frac{1}{T_z} = 0, \quad \frac{1}{T_{x,y}} = \tau^*(E) \overline{\Omega_z^2} \quad (14)$$

It is immediately apparent from Eq. (14) that for electrons injected with their spins aligned along the axis of the wire, there will be no DP relaxation. Spins aligned in the x - y plane will relax. In order to calculate the energy dependent time constant, $\tau^*(E)$, we again substitute into Eq. (7).

$$\begin{aligned} \sum_{\mathbf{k}'} W_{\mathbf{k}\mathbf{k}'}^{abs} & \left\{ (n+1) \frac{f_0(E + \hbar\omega)}{f_0(E)} \tau^*(E) \right. \\ & \left. - n \frac{f_0(E)}{f_0(E + \hbar\omega)} \frac{k'_z (K_{i'}^2 - \Lambda_{j'}^2)}{k_z (K_i^2 - \Lambda_j^2)} \tau^*(E') \right\} \\ & + \sum_{\mathbf{k}''} W_{\mathbf{k}\mathbf{k}''}^{em} \left\{ n \frac{f_0(E - \hbar\omega)}{f_0(E)} \tau^*(E) - (n+1) \right. \\ & \left. \times \frac{f_0(E)}{f_0(E - \hbar\omega)} \frac{k''_z (K_{i''}^2 - \Lambda_{j''}^2)}{k_z (K_i^2 - \Lambda_j^2)} \tau^*(E'') \right\} = 1. \quad (15) \end{aligned}$$

where $k'_z(k''_z)$ is the scattered wave vector for absorption (emission).

The effective time constants are obtained from the coupled equations as for the quantum well case Eq. (12) with the collision integrals now given by $A''(E)$, $B''(E)$, and $C''(E)$ (see the Appendix).

V. RESULTS

Spin-relaxation rates were also calculated for the Elliott-Yafet^{16,17} mechanism. The relaxation times are so long as compared with those of the DP mechanism that, as for the bulk, we neglect the Elliott-Yafet mechanism in the context of polar-optical phonon scattering in intrinsic GaAs over our chosen temperature range. We have also confirmed that a bulk phonon spectrum is sufficient to describe the interaction by comparing results using confined phonon spectra such as the DC (dielectric continuum) model. Effective scattering times, τ^* were calculated using the ladder method, the resulting time constants were compared with those obtained from an analytic solution employing four rungs. There being little discrepancy in the two methods, we have used the simpler analytic solution throughout.

Calculations of the electron spin-relaxation rates in the conduction band (assumed to be parabolic) of nondegenerate

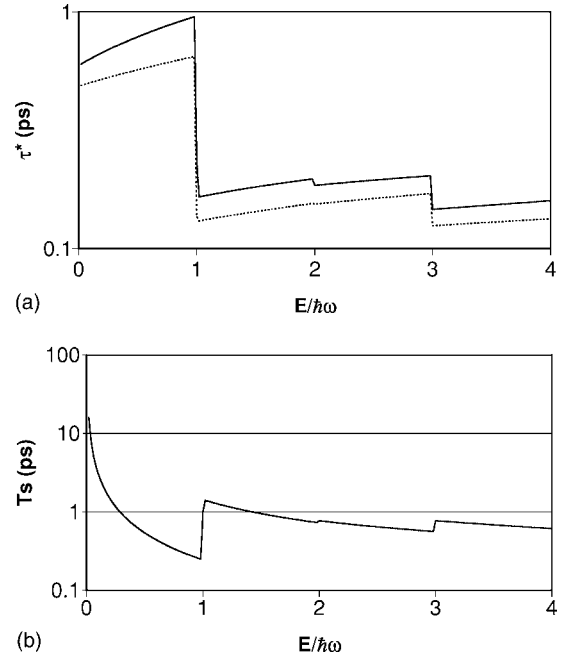


FIG. 1. Spin relaxation in a 5 nm GaAs quantum well (QW) at 300 K via the DP mechanism. (a) Effective scattering time associated with the POP interaction. Solid curve τ_1 , dash curve τ_3 . (b) Spin-relaxation time.

GaAs used the room-temperature data given in Blakemore¹⁸ (Table I) and the estimate for the matrix element, B , given by Fishman and Lampel¹⁴ $B = 10\hbar^2/2m$ describing the interaction with the second electron subband. Commonly quoted values in the literature are given in terms of energy $\hbar\gamma$, writing our frequency in terms of energy gives $28 \text{ eV } \text{\AA}^3$. This value is consistent with other reports in the literature for bulk,^{14,19} although the inclusion of many more remote bands has been reported to reduce $\hbar\gamma$ to $19.7 \text{ eV } \text{\AA}^3$.²⁰

The effective scattering time, τ^* , for the DP mechanism was obtained at a given temperature as a function of energy using the first four rungs of the phonon energy ladder. $\hbar\gamma$ is taken to be $28 \text{ eV } \text{\AA}^3$ throughout. Results for a 5 nm quantum well are shown in Fig. 1(a) for 300 K and in Fig. 2(a) for 200 K. Computations were also carried out for temperatures 225, 250, 250, 275, and 325 K. The time constants exhibit a sharp step at $\hbar\omega$ due to the sudden onset of polar-optical phonon emission. Spin-relaxation rates were calculated using Eq. (10) and the corresponding times, T_s , are shown in Figs. 1(b) and 2(b). There is a large difference in magnitude between bulk and 2D spin relaxation times even though the effective scattering times are very similar. The reason for this is the strong dependence of T_s on subband energy.

Thermally averaged rates were computed for each temperature and the corresponding times are shown in Fig. 3. As one might expect, the POP scattering rate decreases toward low temperature as the phonon population decreases, the spin-relaxation time, T_s , also decreases, giving a monotonic dependence on temperature. In practice, the reduction of the DP spin-relaxation time toward low temperatures will be ameliorated by the increasing rôle played by other scattering mechanisms, primarily those associated with piezoelectric scattering, deformation-potential scattering and charged-

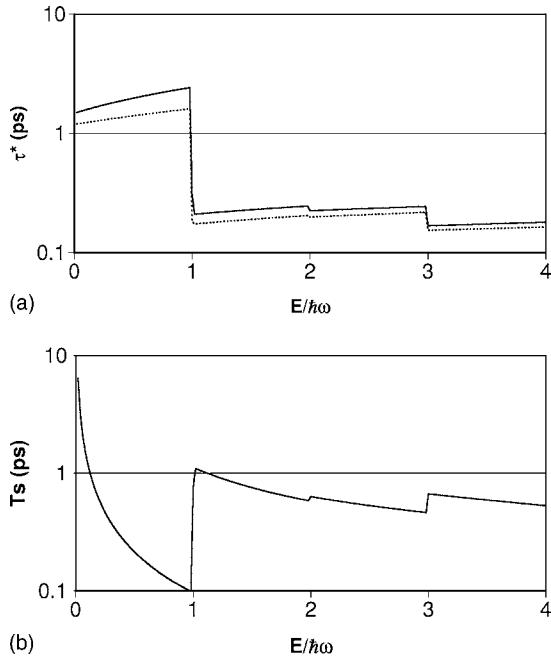


FIG. 2. Spin relaxation in a 5 nm GaAs quantum well (QW) at 200 K via the DP mechanism. (a) Effective scattering time associated with the POP interaction. Solid curve τ_1 , dash curve τ_3 . (b) Spin-relaxation time.

impurity scattering. The effect of any or all of these at room temperature will be to increase the spin-relaxation time via the DP mechanism. The times we quote are, therefore, to be regarded as lower limits.

Thermally averaged rates were also calculated for various well widths. Figure 4 shows the spin-relaxation time against subband energy. The quantum well subband energies are determined by assuming finite $Al_{0.3}Ga_{0.7}As$ barriers. The spin-relaxation time exhibits an E^{-2} dependence on confinement energy in agreement with experiment.^{3,5} For a quantum well with a subband energy, $E_{1e} > kT$ D'Yakonov-Perel predict that the spin-relaxation rate will scale as $\tau_p TE^2$. Our results show that the spin-relaxation time scales as T^2 and the energy-dependent time-constant scales as T^{-3} . Thus our results give the exact same dependencies on temperature and confinement energy as predicted by D'Yakonov-Perel.

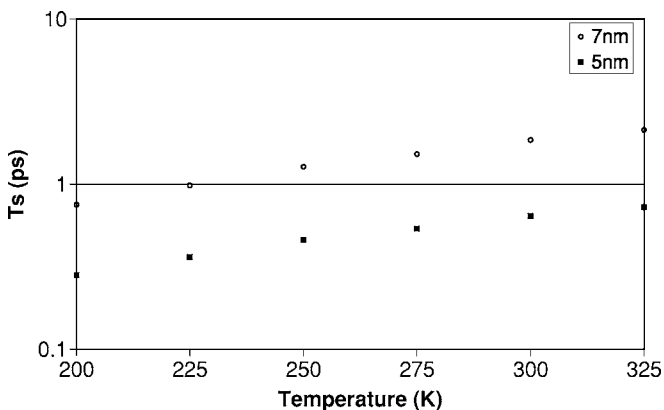


FIG. 3. Temperature dependence in GaAs of the 2D DP spin-relaxation time.

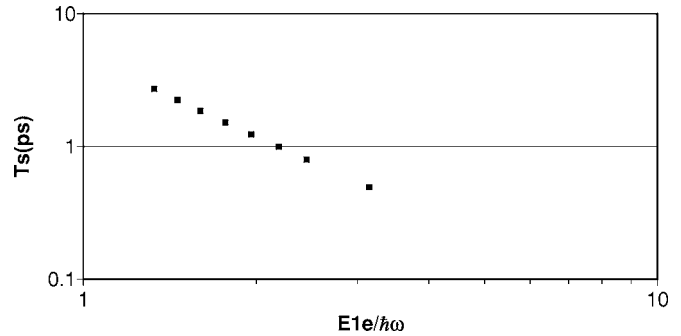


FIG. 4. Subband energy dependence in GaAs QW of the DP spin-relaxation time.

As we have already shown an electron injected with its spin aligned along the axis of the wire will not experience spin relaxation. In addition any orientation of spin will be preserved within a wire of symmetric cross section and with a single subband. First we examined the effect of wire cross-sectional asymmetry on the spin-relaxation time. Wire cross sections of 4 by 4.1 nm to 4 by 7 nm were considered. For simplicity we have limited our study to two subbands; inter-subband scattering becomes possible for a 4 by 4.8 nm cross-section wire. The effective scattering time, τ^* , for the DP mechanism was obtained at a given temperature and wire cross section as a function of energy. Spin-relaxation rates were calculated using Eq. (14). The dramatic effect of cross-

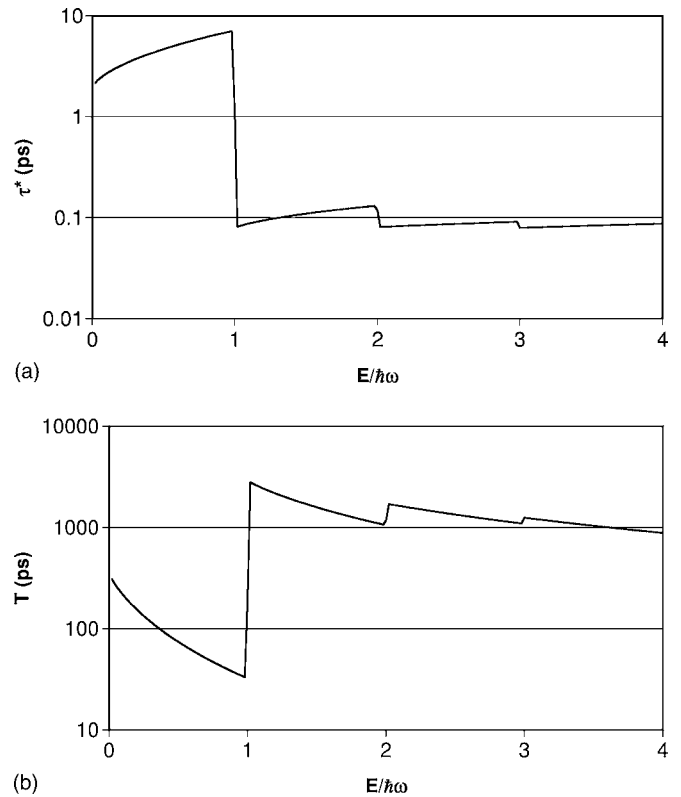


FIG. 5. (a) Variation of effective scattering time with longitudinal energy at 300 K for a quantum wire (QWR) of cross section 4 by 4.1 nm. (b) Variation of spin-relaxation time with longitudinal energy at 300 K for a quantum wire (QWR) of cross section 4 by 4.1 nm.

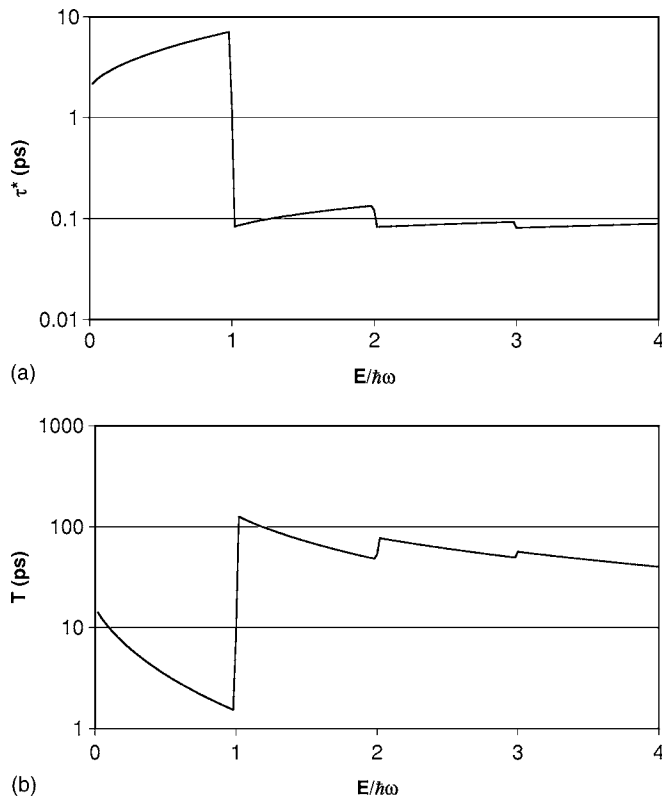


FIG. 6. (a) Variation of effective scattering time with longitudinal energy at 300 K for a quantum wire (QWR) of cross section 4 by 4.5 nm. (b) Variation of spin relaxation time with longitudinal energy at 300 K for a quantum wire (QWR) of cross section 4 by 4.5 nm.

sectional asymmetry on spin relaxation can be seen in Figs. 5 and 6. Figure 5 shows the variation of effective scattering times [Fig. 5(a)] and spin-relaxation times [Fig. 5(b)] with longitudinal energy for a wire of cross section 4 by 4.1 nm. Figure 6, as in Fig. 5, but with a cross section of 4 by 4.5 nm. The time constants exhibit a sharp step at $\hbar\omega$ due to the sudden onset of polar-optical phonon emission. Although the time constants for the two cross sections are identical, since the temperature is the same, the strong dependence on confinement energy results in quite different spin relaxation times.

Figure 7 shows the variation in spin-relaxation time with increasing wire cross section. These times are obtained by performing a thermal average integrating over energy. A Lorentzian level broadening term is introduced to enable integration of the density of states in 1D.²¹ Figure 8(a) shows the variation of the spin-relaxation time with L_x fixed at 4.0 nm while L_y is varied. When the wire is almost symmetric the difference in confinement energies is very small and the resulting spin-relaxation time is very long. For successively more asymmetric wires the spin-relaxation time becomes shorter, eventually becoming quasi-2D when a sufficient number of subbands are considered. T_s scales as L^{-2} . Figure 7(b) shows the same result as Fig. 7(a) but plotted in terms of energy with a log-log scale. T_s varies as the square of the difference between the two subband energies.

Figure 8 shows the temperature dependence of the spin-relaxation time in GaAs. The spin relaxation time decreases

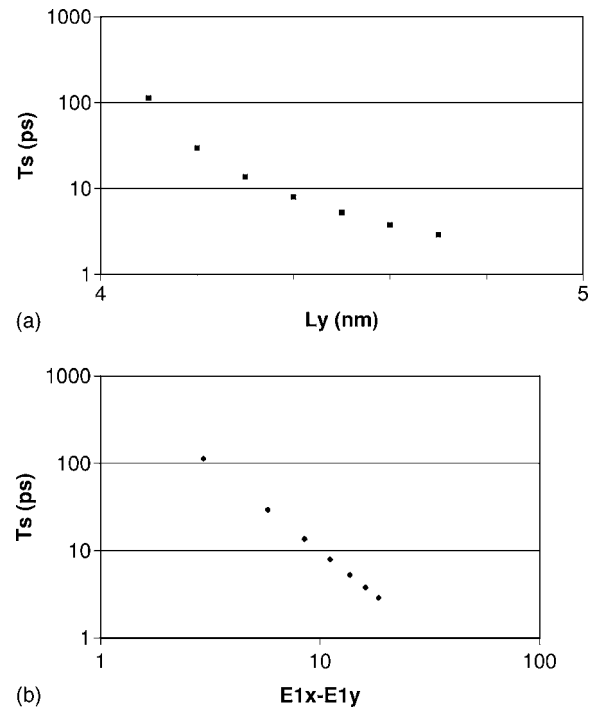


FIG. 7. Variation of spin-relaxation time with QWR cross section at 300 K, $L_x=4$ nm. (a) L_y vs T_s . (b) Difference in subband energies vs T_s .

toward low temperature as the phonon population decreases. In reality this reduction of the DP spin-relaxation time toward low temperature will be balanced by the increasing role played by other scattering mechanisms.

Equation (10) is only valid in the limit $\Omega\tau_p \ll 1$. Figure 9(a) shows the variation of the product $\Omega\tau$ with energy for our temperature range, solid curve 200 K and chain curve 300 K. For all temperatures considered, the relatively large magnitude of the subband energy as compared to the phonon energy results in Ω_1 being on the order of or greater than τ_1 for energies below $\hbar\omega$. In this limit: $\Omega\tau_p > 1$, the spin will relax as Ω_1^{-1} rather than τ_p^{-1} . The product $\Omega_3\tau_3$ is less than one for all temperatures and energies considered. Figure 9(b) shows the variation of the product $\Omega\tau$ with energy for a wire of nearly symmetric cross section and of slightly asymmetric cross section. As in the 2D case the product $\Omega\tau$ becomes large as the phonon emission threshold is reached.

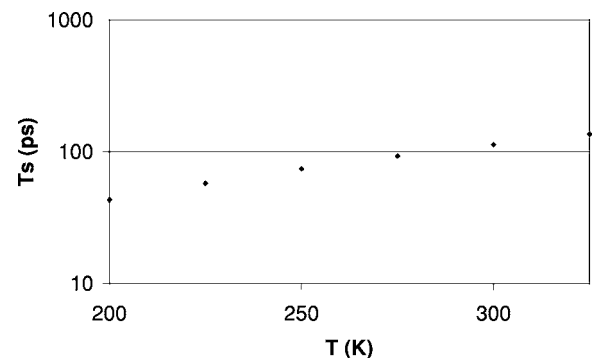


FIG. 8. Temperature dependence of the spin-relaxation time in a QWR of cross section 4 by 4.1 nm.

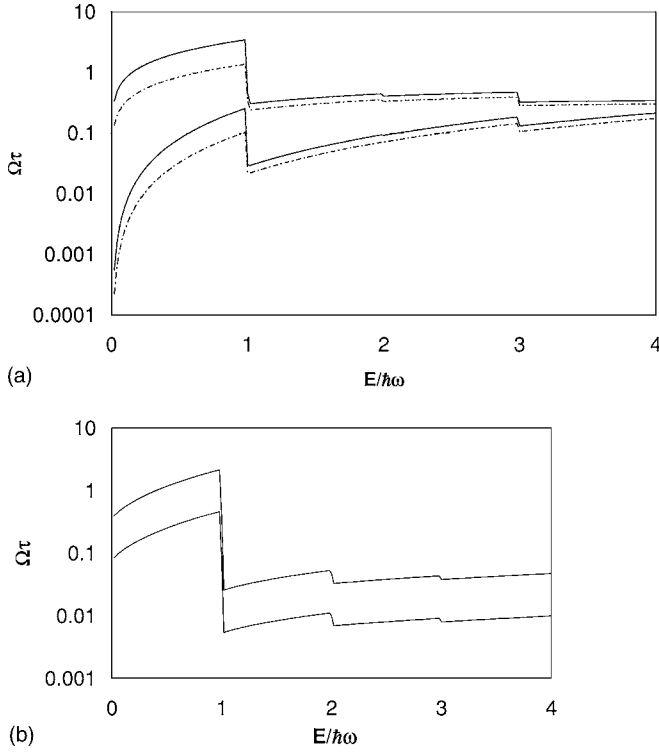


FIG. 9. Energy dependence of the dimensionless quantity $\Omega\tau$ for temperatures of 200 K solid curve and 300 K dashed curve (a) quantum well (b) quantum wire.

It would appear that for low energies spin does not relax via the DP mechanism. However, we must bear in mind that other scattering mechanisms will be present and the rates of these must be added to that of the POP rate in order to obtain an overall energy-dependent time constant.

ACKNOWLEDGMENTS

We are grateful for the support of this work given by the U.S. Office of Naval Research (Grant No. N0014-03-1-0438) sponsored by Dr. Larry Cooper.

APPENDIX: Collision integrals pertaining to Eq. (12)

The scattering rate for the 2D polar-optical-phonon interaction can be expressed as an integral over phonon states with wave vector q in the usual way. Taking account of the conservation of energy and crystal momentum we obtain the integrals that derive from Eq. (12) as follows:

$$A'(E) = -\frac{W_o}{2} \left(\frac{\hbar\omega}{E} \right)^{1/2} n \frac{f_0(E)}{f_0(E+\hbar\omega)} \frac{\Omega'_p}{\Omega_p} \times \int_{q_-^a}^{q_+^a} \frac{F_{11}(q) \cos p\beta'}{q \left[1 - \left(\left(\frac{m\omega}{\hbar k q} \right) + \frac{q}{2k} \right)^2 \right]^{1/2}} dq,$$

$$q_{\pm}^a = k(\sqrt{1 + (\hbar\omega/E)} \pm 1), \quad \cos \beta' = \frac{1 - (q^2/2k^2) + (\hbar\omega/2E)}{\sqrt{1 + (\hbar\omega/E)}}$$

$$\text{QW } F_{11}(q) = \frac{1}{2} \frac{\mu(\mu^2 + \pi^2)(3\mu^2 + 2\pi^2) - \pi^4(1 - e^{-2\mu})}{[\mu(\mu^2 + \pi^2)]^2},$$

$$\mu = \frac{qa}{2}$$

$$\text{SH } F_{11} = \frac{b}{8(q+b)^3} (8b^2 + 9qb + 3q^2)b = \left(\frac{33m^* e^2 N_s}{8\epsilon_s \hbar^2} \right)^{1/3} \quad (\text{A1})$$

For $B'(E)$:

$$B'(E) = W_o \left(\frac{\hbar\omega}{E} \right)^{1/2} \frac{1}{2} \left[\begin{aligned} & (n+1) \frac{f_0(E+\hbar\omega)}{f_0(E)} \int_{q_-^a}^{q_+^a} \frac{F_{11}(q) dq}{q \left[1 - \left(\left(\frac{m\omega}{\hbar k q} \right) + \frac{q}{2k} \right)^2 \right]^{1/2}} \\ & + n \frac{f_0(E-\hbar\omega)}{f_0(E)} \int_{q_-^e}^{q_+^e} \frac{F_{11}(q) dq}{q \left[1 - \left(\left(\frac{m\omega}{\hbar k q} \right) - \frac{q}{2k} \right)^2 \right]^{1/2}} \end{aligned} \right] \quad (\text{A2})$$

and the second term in $B'(E)$ is zero if $E < \hbar\omega$. Finally, for $C'(E)$ we have:

$$C'(E) = -\frac{W_o}{2} \left(\frac{\hbar\omega}{E} \right)^{1/2} [n+1] \frac{f_0(E)}{f_0(E-\hbar\omega)} \frac{\Omega''_p}{\Omega_p} \times \int_{q_-^e}^{q_+^e} \frac{F_{11}(q) \cos p\beta''}{q \left[1 - \left(\left(\frac{m\omega}{\hbar k q} \right) - \frac{q}{2k} \right)^2 \right]^{1/2}} dq,$$

$$q_{\pm}^e = k(1 \pm \sqrt{1 - (\hbar\omega/E)}), \quad \cos \beta'' = \frac{1 - (q^2/2k^2) - (\hbar\omega/2E)}{\sqrt{1 - (\hbar\omega/E)}} \quad (\text{A3})$$

For $E < \hbar\omega$, $C'(E) = 0$. The basic rate is

$$W_o = (e^2/4\pi\hbar\epsilon_p)(2m^*\omega/\hbar)^{1/2}$$

$$\varepsilon_p^{-1} = (\varepsilon_\infty^{-1} - \varepsilon_s^{-1}) \quad (\text{A4})$$

and p takes values of 1 and 3.

Similarly for the 1D polar-optical-phonon interaction: For $A''(E)$:

$$A''(E) = -W_0 n \frac{f_0(E)}{f_0(E + \hbar\omega)} \left(\frac{E + \hbar\omega}{E} \right)^{1/2} \times \int \frac{1}{2} \left(\frac{\hbar\omega}{E + \hbar\omega} \right)^{1/2} \left[\frac{qF(q, n, m)}{q^2 + Q_{a+}^2} + \frac{qF(q, n, m)}{q^2 + Q_{a-}^2} \right] dq \quad (\text{A5})$$

For $B''(E)$:

$$B''(E) = W_0(n+1) \frac{f_0(E + \hbar\omega)}{f_0(E)} \times \int \frac{1}{2} \left(\frac{\hbar\omega}{E + \hbar\omega} \right)^{1/2} \left[\frac{qF(q, n, m)}{q^2 + Q_{a+}^2} + \frac{qF(q, n, m)}{q^2 + Q_{a-}^2} \right] dq + W_0 n \frac{f_0(E - \hbar\omega)}{f_0(E)}$$

$$\times \int \frac{1}{2} \left(\frac{\hbar\omega}{E - \hbar\omega} \right)^{1/2} \left[\frac{qF(q, n, m)}{q^2 + Q_{e+}^2} + \frac{qF(q, n, m)}{q^2 + Q_{e-}^2} \right] dq \quad (\text{A6})$$

and the second term in $B(E)$ is zero if $E < \hbar\omega$. Finally, for $C''(E)$ we have:

$$C''(E) = -W_0(n+1) \frac{f_0(E)}{f_0(E - \hbar\omega)} \left(\frac{E - \hbar\omega}{E} \right)^{1/2} \times \int \frac{1}{2} \left(\frac{\hbar\omega}{E - \hbar\omega} \right)^{1/2} \left[\frac{qF(q, n, m)}{q^2 + Q_{e+}^2} + \frac{qF(q, n, m)}{q^2 + Q_{e-}^2} \right] dq \quad (\text{A7})$$

For $E < \hbar\omega$, $C''(E) = 0$ where

$$F(q, n, m) = G_{n, n'}^2(q_x) G_{m, m'}^2(q_y)$$

$$G_{r, r'}^2(q_\alpha) = (\pi^2 r r')^2 \frac{(q_\alpha L_\alpha / 2)^2 \sin^2(q_\alpha L_\alpha / 2 + (\pi/2)(r + r'))}{[(q_\alpha L_\alpha / 2)^2 - (\pi^2/4)(r - r')^2]^2 [(q_\alpha L_\alpha / 2)^2 - (\pi^2/4)(r + r')^2]^2} \quad (\text{A8})$$

with

$$Q_{e\pm} = Q_0(\sqrt{E \mp \hbar\omega})$$

$$Q_{a\pm} = Q_0(-\sqrt{E \pm \hbar\omega}) \quad (\text{A9})$$

for forward and backward scattering.

¹M. I. D'yakonov and V. I. Perel, *Sov. Phys. Solid State* **13**, 3023 (1972) [*Fiz. Tverd. Tela (Leningrad)* **13**, 3581 (1972)].

²M. I. D'yakonov and V. Yu. Kachorovskii, *Sov. Phys. Semicond.* **20**, 110 (1986) [*Fiz. Tekh. Poluprovodn. (S.-Peterburg)* **20**, 178 (1986)].

³A. Tackeuchi, Y. Nishikawa, and O. Wada, *Appl. Phys. Lett.* **68**, 797 (1996).

⁴R. Terauchi *et al.* *Jpn. J. Appl. Phys., Part 1* **38**, 2549 (1999).

⁵A. Malinowski *et al.* *Phys. Rev. B* **62**, 13034 (2000).

⁶S. Pramanik, S. Bandyopadhyay, and M. Cahay, *cond-mat/0403021* (2004).

⁷A. A. Kiselev and K. W. Kim, *Phys. Rev. B* **61**, 13115 (2000).

⁸S. Pramanik, S. Bandyopadhyay, and M. Cahay, *Phys. Rev. B* **68**, 075313 (2003).

⁹R. T. Delves, *Proc. Phys. Soc. London* **73**, 572 (1959).

¹⁰K. Fletcher and P. N. Butcher, *J. Phys. C* **5**, 212 (1972).

¹¹B. K. Ridley, *J. Appl. Phys.* **84**, 4020 (1998).

¹²D. R. Anderson, N. A. Zakhleniuk, M. Babiker, B. K. Ridley, and C. R. Bennett, *Phys. Rev. B* **63**, 245313 (2001).

¹³A. Dyson and B. K. Ridley, *Phys. Rev. B* **69**, 125211 (2004).

¹⁴G. Fishman and G. Lampel, *Phys. Rev. B* **16**, 820 (1977).

¹⁵G. E. Pikus and A. N. Titkov, *Optical Orientation* (Elsevier, New York, 1984) p. 73.

¹⁶R. J. Elliott, *Phys. Rev.* **96**, 266 and 280 (1954).

¹⁷Y. Yafet, *Solid State Phys.* **14**, 1 (1963).

¹⁸J. S. Blakemore, *J. Appl. Phys.* **53**, R 123 (1982).

¹⁹F. G. Pikus and G. E. Pikus, *Phys. Rev. B* **51**, 16928 (1995).

²⁰J. Kainz, U. Rossler, and R. Winkler, *Phys. Rev. B* **68** 075322 (2003).

²¹H. Sakaki, K. Kato, and H. Yoshimura, *Appl. Phys. Lett.* **57** 2800 (1990).